Biochem. J. (1988) 251, 527–540 (Printed in Great Britain)

Kinetic trapping of intermediates of the scallop heavy meromyosin adenosine triphosphatase reaction revealed by formycin nucleotides

Andrew P. JACKSON and Clive R. BAGSHAW*
Department of Biochemistry, University of Leicester, Leicester LE1 7RH, U.K.

The kinetics of interaction of formycin nucleotides with scallop myosin subfragments were investigated by exploiting the fluorescence signal of the ligand. Formycin triphosphate gives a 5-fold enhancement of the emission intensity on binding to heavy meromyosin, and the profile indicates that the kinetics of binding are Ca^{2+}-insensitive. In contrast, the subsequent product-release steps show a marked degree of regulation by Ca^{2+}. In the absence of Ca^{2+} formycin triphosphate turnover by the unregulated and the regulated heavy meromyosin fractions are clearly resolved, the latter showing a fluorescence decay rate of $0.002\ s^{-1}$, corresponding to the P_i-release step. In the presence of Ca^{2+} this step is activated 50-fold. Formycin diphosphate release is also regulated by Ca^{2+}, being activated from $0.008\ s^{-1}$ to $5\ s^{-1}$. In contrast with protein tryptophan fluorescence [Jackson & Bagshaw (1988) Biochem. J. **251**, 515–526], formycin fluorescence is sensitive to conformational changes that occur subsequent to the binding step and demonstrate, directly, an effect of Ca^{2+} on both forward and reverse rate constants. Apart from a decrease in the apparent second-order association rate constants, formycin derivatives appear to mimic adenosine nucleotides closely in their interaction with scallop heavy meromyosin and provide a spectroscopic handle on steps that are optically silent with respect to protein fluorescence. A novel mechanism is discussed in which regulation of the formycin triphosphate activity by Ca^{2+} involves kinetic trapping of product complexes.

INTRODUCTION

The characterization of the elementary steps of the scallop striated adductor myosin ATPase reaction by using changes in the protein tryptophan fluorescence is limited by the rather small enhancements observed on nucleotide binding (Jackson & Bagshaw, 1988). Furthermore, a key step in the pathway, that of P_i release, is accompanied by little or no (less than 2%) change in tryptophan fluorescence (Wells *et al.*, 1985). As a result, this signal cannot be used to monitor the extreme Ca^{2+}-sensitivity of the product-release steps known to occur from discontinuous assay procedures (Wells & Bagshaw, 1985). Fluorescent ATP analogues provide a means of increasing the amplitudes of the optical signals associated with the elementary steps of the ATPase reaction. In particular, formycin nucleotides have found wide application in biological systems (Ward *et al.*, 1969*b*; Rossomando *et al.*, 1981). On binding to rabbit skeletal-muscle and other myosin subfragments, FTP shows a large enhancement in fluorescence, followed by a decrease in signal concomitant with product release (Bagshaw *et al.*, 1972; White *et al.*, 1986). FTP supports contraction of glycerinated vertebrate skeletal muscle (Ferenczi, 1978) and scallop striated adductor muscle (A. P. Jackson & C. R. Bagshaw, unpublished work).

ATP analogues have also been devised with a modified phosphate chain as a means of preventing or perturbing the hydrolytic step (Yount *et al.*, 1971; Trentham *et al.*, 1976). Such analogues have been used to characterize the kinetics of the nucleotide-binding steps of rabbit skeletal-muscle myosin (Bagshaw *et al.*, 1974; Trybus & Taylor, 1982). p[NH]ppF was therefore synthesized as a probe for the nucleotide-binding and -release steps of scallop HMM. In the present study it is shown that formycin nucleotides provide sensitive probes to differentiate and characterize the rate constants of the elementary steps of a heterogenous population of regulated and unregulated scallop HMM. In addition, these analogues have revealed a novel feature of the enzymic mechanism whereby product complexes become trapped in a refractory state in the absence of Ca^{2+}. These intermediates appear to be fundamental to the mechanism of relaxation of molluscan muscle.

MATERIALS AND METHODS

Materials

Proteins were prepared as referenced in the accompanying paper (Jackson & Bagshaw, 1988). FTP and FDP were prepared by the enzymic method of Rossomando *et al.* (1981). p[NH]ppF was synthesized by a method analogous to that of Rodbell *et al.* (1971), with use of the exchange reaction of PP_i and sodium imidodiphosphate as catalysed by a crude preparation of amino acid-activating enzymes (S-100). The latter was obtained by lysing 40 g of fresh or frozen baker's-yeast cells in 70 ml of 60 mM-KCl/14 mM-$MgCl_2$/6 mM-2-mercaptoethanol/10 mM-Tris/HCl buffer, pH 8.0, in a

Abbreviations used: p[NH]ppA, adenosine 5′-[$\beta\gamma$-imido]triphosphate; Ap_5A, P^1P^5-di(adenosine-5′)-pentaphosphate; FDP, formycin A 5′-diphosphate; FMP, formycin A 5′-monophosphate; FTP, formycin A 5′-triphosphate; p[NH]ppF, formycin A 5′-[$\beta\gamma$-imido]triphosphate; HMM, heavy meromyosin; S1, subfragment 1; $S1^{-RD}$, subfragment 1 lacking regulatory domain; f.p.l.c., fast protein liquid chromatography.

* To whom correspondence should be addressed.

French press. After centrifuging at 30000 *g* for 60 min to remove cell debris, the supernatant was dialysed against the same buffer for 4 h at 4 °C. The extract was then centrifuged at 100000 *g* for 2 h and the supernatant (S-100) was rapidly frozen and stored at −70 °C. Yeast proved to be a better source of S-100 than *Escherichia coli*, which had been used previously (Rodbell *et al.*, 1971; Bagshaw, 1974), because large quantities of DNA were not released into the supernatant during the lysis of the cells. To carry out the exchange reaction, the yeast S-100 extract was incubated in medium containing 3 mM-FTP, 12 mM-sodium imidodiphosphate (Sigma Chemical Co.), 15 mM-$MgCl_2$, 140 mM-Tris/HCl buffer, pH 7.6, and a mixture of coded amino acids (0.4 mM each except lysine) for 1 h at 20 °C. The reaction was terminated by boiling for 3 min. After cooling, adenylate kinase (25 units/ml; Sigma Chemical Co.) and rabbit myosin S1 (2.5 μM) were added and the mixture was left for 16 h at room temperature to convert any unchanged FTP into FMP. The yield of p[NH]ppF (10%) was less than that of p[NH]ppA (60%) prepared by the same method. It is probable that FTP reacts more slowly with the amino acid-activating enzymes, allowing phosphatase reactions to compete. p[NH]ppF was purified by ion-exchange chromatography on a DEAE-Sephadex A-25 column (1 cm × 25 cm) with a gradient of 0.1–0.7 M-triethylamine bicarbonate at pH 7.5. The peak fractions were concentrated to an oil by rotary evaporation with ethanol and analysed on a Mono Q f.p.l.c. column (Pharmacia) with a gradient of 0–1 M-NaCl in 20 mM-Bis/Tris buffer, pH 6.5. p[NH]ppF was eluted as a single peak between the FDP and FTP standards, analogous to the relative position of p[NH]ppA with respect to ADP and ATP.

Spectroscopic methods

Manual and stopped-flow fluorescence measurements were performed with the apparatus described in the accompanying paper (Jackson & Bagshaw, 1988). Formycin fluorescence was excited at 313 nm. This wavelength corresponds to an Hg line that is reasonably clear of protein fluorescence excitation. At stoichiometric protein/formycin ratios the contribution from the tryptophan to the observed emission intensity at 350 nm was less than 15%. The concentration of formycin nucleotides was calculated by using ϵ_{295} 9950 $M^{-1} \cdot cm^{-1}$ (Ward *et al.*, 1969*a*).

E.p.r. measurements were carried out with a Varian E109 spectrometer (Wells & Bagshaw, 1983).

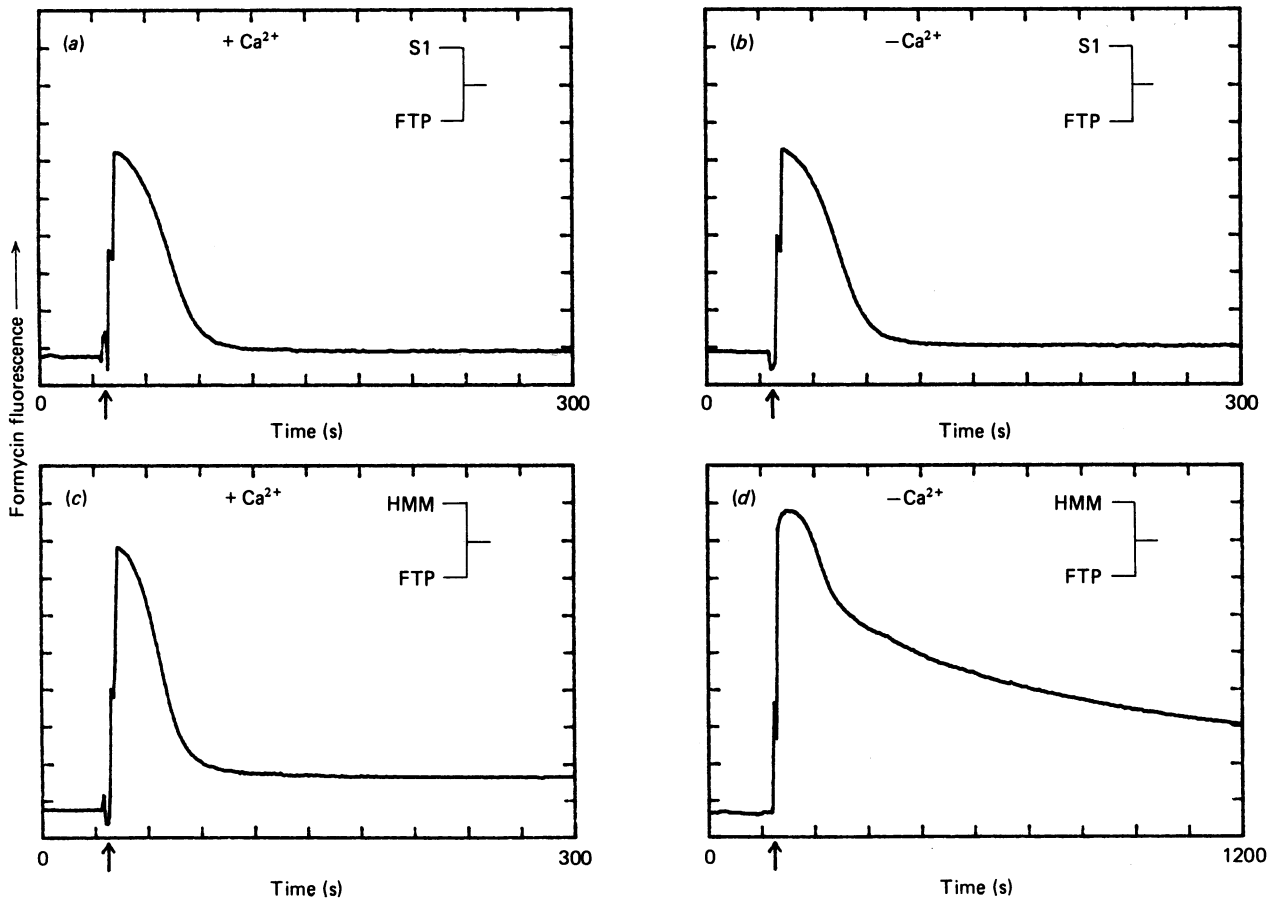

Fig. 1. FTP turnover by $S1^{-RD}$ and HMM

Formycin fluorescence was monitored on manual addition of FTP to the protein in a standard 1 cm-pathlength cell by using a Baird–Atomic SFR fluorimeter. (*a*) 10 μM-FTP was added to 2 μM-$S1^{-RD}$ in the presence of 100 μM-Ca^{2+}. (*b*) As (*a*), but in the presence of 100 μM-EGTA. (*c*) 10 μM-FTP was added to 2 μM-HMM in the presence of 100 μM-Ca^{2+}. (*d*) as (*c*), but in the presence of 100 μM-EGTA. Reactions were carried out in buffer containing 20 mM-NaCl, 1 mM-$MgCl_2$ and 10 mM-Tes at pH 7.5 and 20 °C. ↑denotes the time of addition of the FTP. The slow phase of (*d*) fitted to a rate constant of 0.0018 s^{-1}.

Discontinuous assays

All assays were carried out in a buffer containing 20 mM-NaCl, 1 mM-$MgCl_2$ and 10 mM-Tes at pH 7.5 and 20 °C, unless otherwise stated. FTPase activity was measured from the rate of appearance of P_i as determined by using the Malachite Green assay (Itaya & Ui, 1966). Alternatively, the reaction was monitored by following the conversion of FTP into FDP by using fast ion-exchange chromatography. The reaction mixture was quenched with $HClO_4$ and neutralized, as described by Bagshaw & Trentham (1973). The products were separated by a Mono Q f.p.l.c. column with a 0–1 M-NaCl gradient in 20 mM-Bistris buffer, pH 6.5. The elution profiles were captured by using a 12-bit A/D converter coupled to an Apple II+ microcomputer, and the progress of the reaction was determined from the area under the FDP and FTP peaks. This procedure also revealed the production of FMP under some conditions, presumably as a result of adenylate kinase activity. Ap_5A (10 μM) was added to the assay mixtures to minimize this side reaction.

RESULTS

FTP turnover

Formycin fluorescence is enhanced about 5-fold when FTP is bound to scallop myosin subfragments during the steady-state turnover. Figs. 1(*a*) and 1(*b*) show that the turnover time of a limited molar excess of FTP by $S1^{-RD}$ is independent of Ca^{2+}. The period of enhanced fluorescence indicated that the steady-state rate of the FTPase activity is about 0.15 s^{-1} (cf. ATP turnover, 0.3 s^{-1}; Wells *et al.*, 1985; Jackson & Bagshaw, 1988). At the end of the reaction the fluorescence intensity returned almost to its initial value, suggesting that the product FDP is bound very weakly and/or the bound FDP exhibits little fluorescence enhancement over free FDP.

The turnover of FTP by HMM, in the presence of Ca^{2+}, showed a very similar profile to that of S1 (Fig. 1*c*). However, in the absence of Ca^{2+} the profile was markedly different (Fig. 1*d*). The brief steady-state phase was prolonged by about 3-fold, and the subsequent decay in fluorescence was markedly biphasic. About one-third of the fluorescence enhancement recovered quickly, but the remainder decayed exponentially with a rate constant of

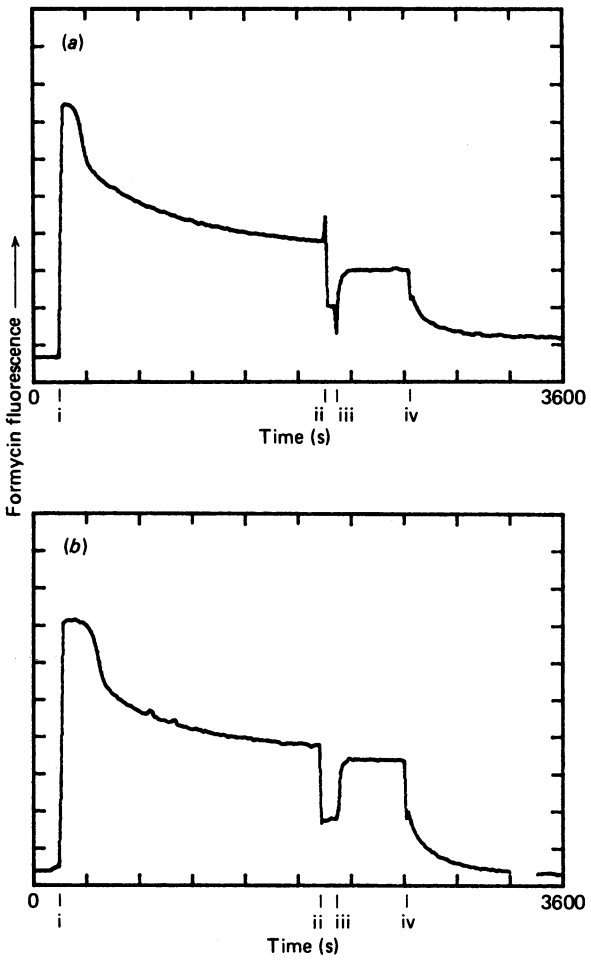

Fig. 2. Multiple turnovers of FTP by HMM showing product FDP binding

Formycin fluorescence was recorded as described in Fig. 1 legend in a buffer initially containing 100 μM-EGTA. (*a*) The following components were added to 10 μM-FTP at the times indicated: i, 2 μM-HMM; ii, 200 μM-$CaCl_2$; iii, 200 μM-EGTA; iv, 1 mM-MgATP. (*b*) As (*a*), but 20 μM-FTP was present initially. Note the increased turnover time of the first phase and the increased amplitude associated with FDP re-binding in (*b*). The data are analysed in detail in Table 1.

Table 1. Fluorescence amplitudes and calculated rate constants for FTP turnover by HMM in the absence and in the presence of Ca^{2+}

[FTP] (μM)	Ca^{2+}	Relative amplitudes*			Rates (s^{-1})			
		Fast phase	Slow phase	End point	Turnover time of fast phase(s)	Observed steady state †	Unregulated steady state‡	Regulated single turnover
10	–	0.30	0.50	0.20	132	0.038	0.13	0.0014
20	–	0.32	0.32	0.36	240	0.041	0.13	0.0017
10	+	0.87	–	0	48	0.10	–	–
20	+	0.84	–	0	87	0.11	–	–

* Relative to total observed change in the absence of Ca^{2+}, with the end point in the presence of Ca^{2+} as a baseline.

† Calculated from the turnover time of the FTP by a total of 2 μM-HMM (nominal added concentration).

‡ Corrected rate assuming steady-state turnover is due entirely to unregulated fraction (estimated from amplitude of the fast phase).

$0.0018\ s^{-1}$. The overall profile of the reaction was very similar to that of the turbidity change observed during the turnover of ATP by acto-(scallop HMM) (Wells & Bagshaw, 1984*a*) and appears to have a similar basis. Increasing the added FTP concentration at fixed [HMM] caused a proportional increase in the turnover time of the fast phase, whereas the rate of the slow phase was little affected (Fig. 2 and Table 1). Thus most of the FTP is hydrolysed by the unregulated fraction during its brief steady-state phase, and the regulated fraction effectively undergoes a single turnover. The fraction of unregulated molecules can be estimated from the amplitude of the fast phase relative to the total change. (The latter was measured by using the final fluorescence value in the presence of Ca^{2+} as a baseline rather than the initial value of the free FTP, which is perturbed on addition of HMM by the contribution from tryptophan fluorescence.) The average amplitude of the fast phase of decay, in 16 preparations, was 28% (S.D. 7.1%) of the total fluorescence enhancement. If the observed steady-state rate of the preparation in Fig. 2 in the absence of Ca^{2+} ($0.04\ s^{-1}$) is attributed exclusively to this minor fraction, then the rate corrected on a per-site basis ($0.13\ s^{-1}$) is close to that of the observed rate for the whole population in the presence of Ca^{2+} ($0.11\ s^{-1}$; Table 1), thus justifying the description of this fraction as being unregulated.

Although the rate of the slow phase of the decay in formycin fluorescence in the absence of Ca^{2+} was unaffected by increasing [FTP], as expected for a first-order reaction, the observed amplitude was diminished because of the increased amount of FDP that remained bound at the end of the reaction (Table 1). This was demonstrated by addition of Ca^{2+} to the reaction mixture, at a time when the turnover was almost complete, to give the baseline fluorescence (the operational definition), followed by addition of excess EGTA, which caused the product FDP to re-bind (Fig. 2). The amplitude of the fluorescence enhancement associated with the FDP binding increased as a function of the initial FTP added (and hence the [FDP] generated). The kinetics of FDP binding is discussed further below. Recording FTP turnovers with either 1 mm or 5 mm excitation slit widths had no effect on the rate of the slow phase, indicating that photodecomposition was not a severe problem in this measurement.

The turnover time of the fast phase of formycin fluorescence during FTP hydrolysis of HMM showed about a 3-fold sensitivity to Ca^{2+} (Figs. 1*c* and 1*d* and Table 1), as noted for ATP turnover monitored by tryptophan fluorescence (Wells *et al.*, 1985). However, when the steady-state turnover of FTP was monitored over 10 min, by assaying the production of P_i, the rate (0.12 mol of P_i/s per mol of HMM heads) showed little dependence of Ca^{2+}. This anomalous behaviour appeared to be due to a small (2–3-fold) activating effect of FDP, which accumulated during prolonged FTP turnover, on the unregulated fraction. The precise mechanism for this effect, which has not been observed with ADP, is unclear. The key result, however, which is evident from the fluorescence profiles of FTP under limited turnover conditions (Figs. 1*c* and 1*d*), is that Ca^{2+} markedly activates (> 50-fold) the regulated HMM fraction and this constitutes the majority of the preparation.

The rate constant of the slow fluorescence decay in Fig. 1(*d*) is very similar to that of the P_i-release step when ATP is used as substrate (Wells & Bagshaw, 1985).

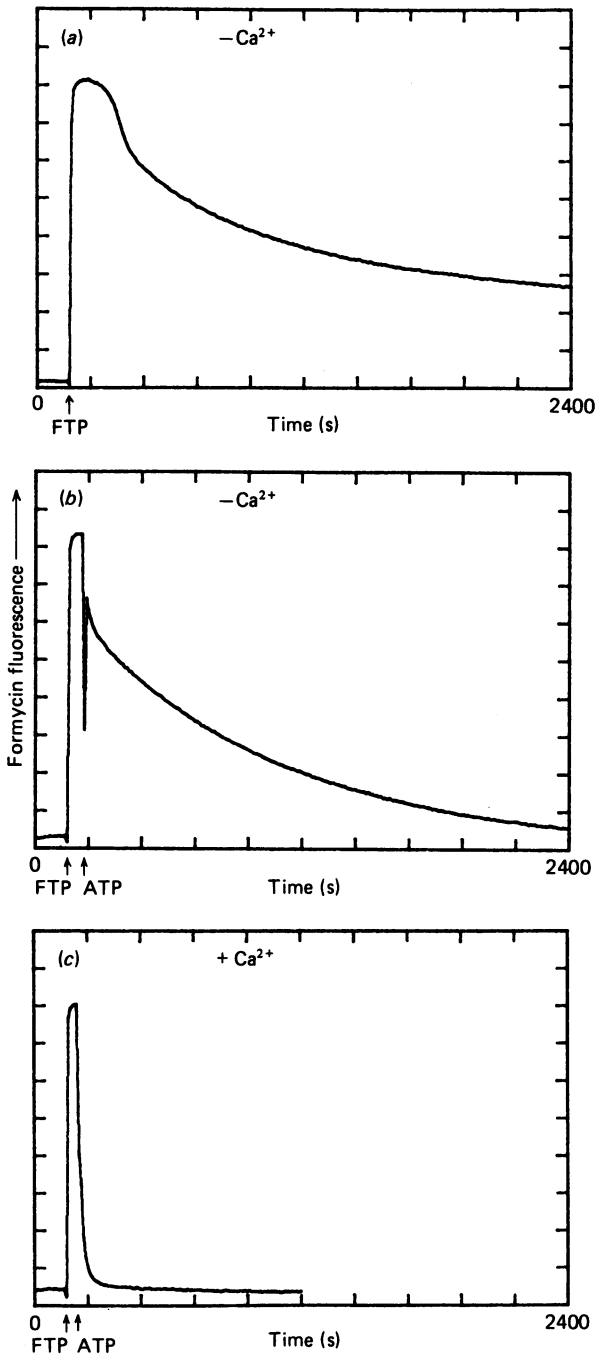

Fig. 3. FTP turnover by HMM chased with ATP

Formycin fluorescence was recorded as described in Fig. 1 legend. (*a*) 10 μM-FTP was added to 2 μM-HMM in the presence of 100 μM-EGTA. An exponential fit to the slow phase yielded a rate constant of $1.4 \times 10^{-3}\ s^{-1}$. (*b*) As (*a*), but after 80 s 1 mM-MgATP was added. The rate of the slow phase was unaffected ($1.3 \times 10^{-3}\ s^{-1}$), but its total amplitude was increased owing to the displacement of bound FDP. (*c*) As (*a*), but after 60 s 200 μM-Ca^{2+} and 1 mM-MgATP were added.

By analogy, it seemed likely that $M \cdot FDP \cdot P_i$ is the major steady-state intermediate that gave rise to the enhanced formycin fluorescence and that P_i dissociation is the rate-limiting step. To explore this conclusion further, stoichiometric FTP and HMM were mixed and the reaction was quenched with $HClO_4$ after 5 s, when FTP binding

was complete. Analysis of the nucleotide released, by f.p.l.c., revealed that more than 80% of the nucleotide was FDP, both in the presence and in the absence of Ca^{2+}. Thus the hydrolysis step is rapid relative to the product-release step, the residual FTP (10–20%) probably being a consequence of the equilibrium position of the hydrolysis step (Bagshaw & Trentham, 1973). These results support the proposal that the enhanced formycin fluorescence state corresponds to an HMM–product complex.

The presence of an unregulated fraction of HMM, which behaves like S1, has demanded the use of single-turnover or limited-turnover experiments to reveal the kinetics of the regulated HMM fraction (Wells & Bagshaw, 1984*a*, 1985; Jackson *et al.*, 1986). One criticism of this approach is that the final turnover of the HMM ATPase might be atypical in some way and that it does not represent the physiological conditions of relaxation, where there is a vast excess of ATP over the myosin head concentration. A double-mixing experiment was performed to examine the influence of excess ATP on the turnover of the nucleotide by the regulated HMM fraction.

A 5-fold molar excess of FTP was added to HMM, manually, in the absence of Ca^{2+}. Once the FTP had bound, 1 mM-MgATP was added (Fig. 3). The fluorescence decay as the formycin nucleotide was displaced from the HMM was markedly biphasic in the absence of Ca^{2+}. The fast phase, corresponding to formycin product release from the unregulated fraction, was too fast to resolve by manual addition. The slow phase had a rate constant of 0.017 s^{-1}, which agreed with the rate constant obtained when FTP was turned over by the regulated fraction without chasing with ATP (Fig. 3*a*; cf. Fig. 3*b*). The amplitude of the slow phase was larger in the chase experiment because product FDP cannot bind in the presence of an excess of ATP. The release of formycin nucleotides on addition of excess ATP in the presence of Ca^{2+} was much faster and was not clearly resolved from the mixing process (Fig. 3*c*). These results demonstrate that the final turnover of nucleotide by HMM is not atypical and thus our conclusions from previous transient-state-kinetic studies appear to hold. The records also rule out any effect of contaminating adenylate kinase in prolonging the slow phase of Fig. 3(*a*), because in Fig. 3(*b*) any regenerated FTP would be unable to bind in the presence of an excess of ATP. Double-mixing stopped-flow experiments are required to resolve the FTP turnover by the unregulated fraction. This approach has the advantage over single or limited turnovers in the absence of an ATP chase in giving a well-defined state to the fluorescence decay rather than the sigmoidal approach observed in Figs. 1 and 3(*a*).

FTP binding

The large enhancement in formycin fluorescence associated with the FTP-binding phase was investigated by stopped-flow methods. The reaction records obtained in the presence and in the absence of Ca^{2+} are almost superimposable (Fig. 4). Increasing the FTP concentration increased the observed pseudo-first-order rate constant and yielded an apparent second-order association constant of 2×10^5 $M^{-1} \cdot s^{-1}$. There was no indication of the observed rate constant levelling off at the highest FTP concentration used (200 μM in the reaction chamber; rate 46 s^{-1}). Higher concentrations of

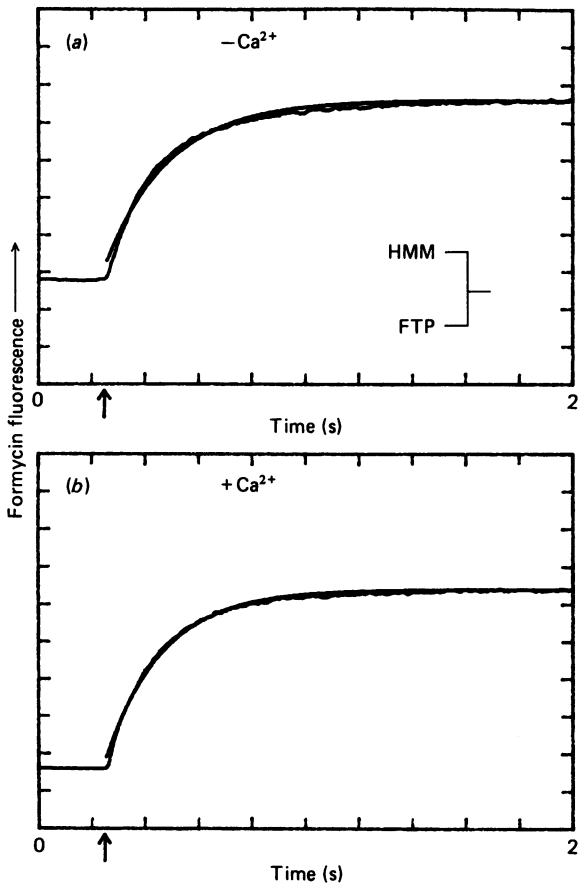

Fig. 4. FTP binding to HMM

The stopped-flow records show FTP binding to HMM monitored by the enhancement in formycin fluorescence. (*a*) 40 μM-FTP was mixed with 4 μM-HMM in the presence of 100 μM-EGTA. (*b*) 40 μM-FTP was mixed with 4 μM-HMM in the presence of 100 μM free Ca^{2+}. Other conditions were as for Fig. 1. Exponential fits, superimposed on the traces, yielded rate constants of (*a*) 4.4 s^{-1} and (*b*) 4.9 s^{-1}. One vertical division represents a 6% change in fluorescence relative to the end point.

FTP were not examined because the background fluorescence of the free FTP would become too high. Thus the 500% fluorescence enhancement observed on FTP binding to HMM under stoichiometric conditions corresponds to only a 5% enhancement when a 100-fold molar excess of FTP is employed. The apparent second-order association rate constant for FTP binding to scallop HMM is an order of magnitude lower than that for ATP binding (Jackson & Bagshaw, 1988).

FDP binding and release

FDP binding to scallop HMM, in the absence of Ca^{2+}, gave a detectable enhancement of formycin fluorescence, but the amplitude was less than that induced by FTP over the concentration range studied (3–75 μM). FDP binding was evident from the elevated fluorescence at the end point of an FTP turnover in the absence of Ca^{2+} (Fig. 2 and Table 1). In those experiments the increase in the amplitude of fluorescence associated with FDP binding with increasing initial [FTP] indicated an FDP binding constant of greater than 10 μM. The rate and amplitude of the fluorescence changes were studied

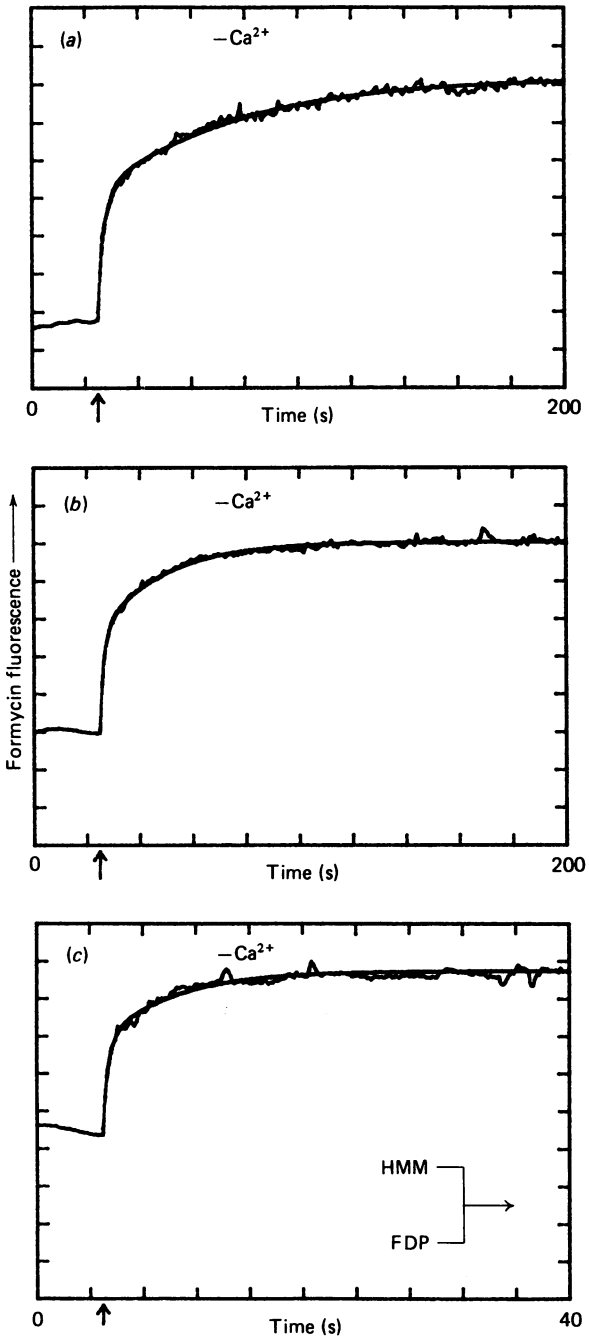

Fig. 5. FDP binding to HMM in the absence of Ca^{2+}

The stopped-flow records show FDP binding to HMM monitored by the enhancement in formycin fluorescence. (*a*) 20 μM-FDP was mixed with 4 μM-HMM. (*b*) 50 μM-FDP was mixed with 4 μM-HMM. (*c*) 150 μM-FDP was mixed with 4 μM-HMM. EGTA (100 μM) was present throughout. Other conditions were as for Fig. 1. Biphasic exponential fits yielded rate constants and relative amplitudes in (*a*) 0.42 s^{-1} (51%) and 0.019 s^{-1} (49%), (*b*) 0.65 s^{-1} (53%) and 0.042 s^{-1} (47%), and (*c*) 2.3 s^{-1} (56%) and 0.19 s^{-1} (44%). The total amplitude of the fluorescence enhancement is shown in Fig. 6 as a function of the reaction-chamber [FDP]. One vertical division represents a 2% change in fluorescence.

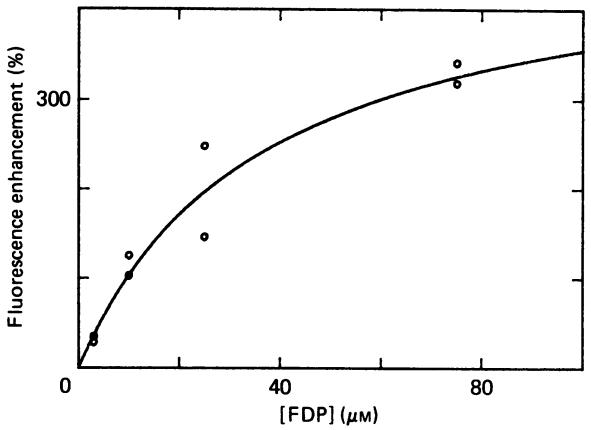

Fig. 6. Enhancement in formycin fluorescence as a function of [FDP]

The amplitudes of the fluorescence enhancement (%) observed in stopped-flow experiments, such as those in Fig. 5, were corrected for background fluorescence attributed to free FDP. The best-fit hyperbola yielded an equilibrium constant of 37 μM and a maximum enhancement of 485% for HMM when saturated with FDP.

further by direct addition of FDP to HMM. A complete analysis proved difficult to perform because increasing [FDP] gave a corresponding increase in the basal fluorescence level, thus decreasing the relative amplitude of the signal of interest. Furthermore, the signals were at least biphasic and only the slowest phase was resolved when additions were performed manually [cf. Fig. 2(*b*), where the re-binding of FDP appears biphasic]. The amplitude of the instantaneous phase when HMM was added manually to FDP cannot be analysed accurately because of difficulties in establishing the true baseline. This was less of a problem in stopped-flow measurements (assuming there was no extremely rapid phase that was complete within the dead-time of 1 ms) where the fast phase was resolved (Fig. 5). However, stopped-flow measurements were still subject to a progressive loss in signal-to-noise ratio with increasing background FDP fluorescence, limiting reaction-chamber concentrations to about 75 μM-FDP. A plot of the total amplitude of the fluorescence change recorded in the stopped-flow apparatus against [FDP], when analysed in terms of a hyperbola, yielded an apparent binding constant of about 40 μM and an extrapolated maximum enhancement of about 5-fold (Fig. 6). The validity of such an analysis is questionable, however, in view of the possibility of two classes of FDP-binding sites (see the Discussion section). The dissection of the fluorescence stopped-flow traces into their constituent phases, across the concentration range studied, was not achieved with high accuracy. Increasing FDP was apparently accompanied by an increase in the observed rate constant for both phases and a small increase in the amplitude of the fast phase relative to the slow phase (Fig. 5).

In the presence of Ca^{2+} FDP addition to HMM caused little change in formycin fluorescence. At high FDP concentrations (above 50 μM) a small enhancement was observed in the stopped-flow apparatus comparable with the fast phase observed in Fig. 5(*c*). However, it was difficult to rule out an instrument artifact. Measurements performed by manual addition require subtraction of the high background fluorescence arising from the free FDP. This could not be achieved with sufficient accuracy to check the validity of the signal observed in the stopped-

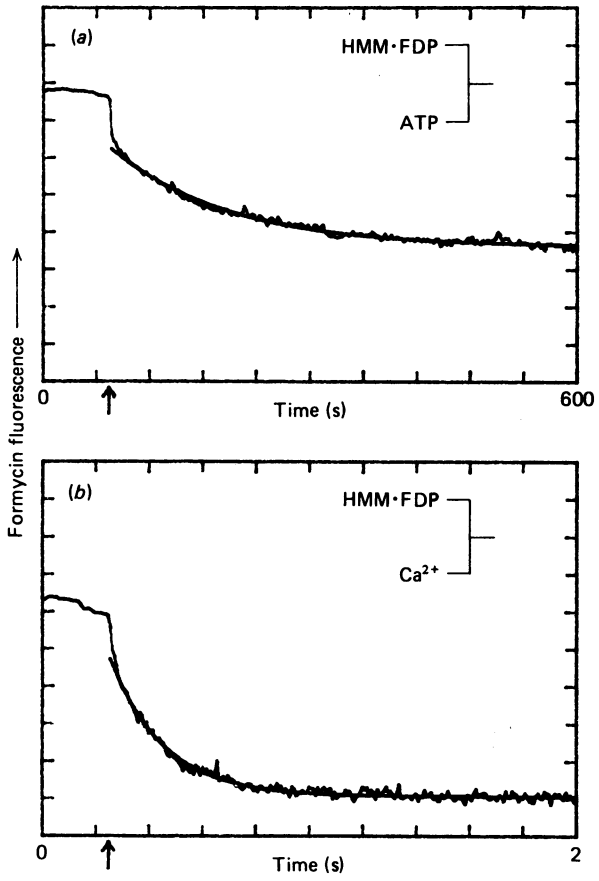

Fig. 7. FDP dissociation from HMM

The stopped-flow records show the dissociation of FDP from HMM in the absence and in the presence of Ca^{2+}, as monitored by formycin fluorescence. (*a*) One syringe contained 500 μM-ATP and the other 4 μM-HMM, 6 μM-FDP and 100 μM-EGTA. (*b*) One syringe contained 200 μM-Ca^{2+} and the other 4 μM-HMM, 6 μM-FDP and 100 μM-EGTA. Other conditions were as for Fig. 1. Exponential fits yield rate constants of (*a*) 0.008 s^{-1} and (*b*) 5.3 s^{-1}. One vertical division represents a 2% change in fluorescence.

flow apparatus. The extent of FDP binding under these conditions therefore cannot be determined by this spectrofluorimetric approach.

FDP dissociation from HMM in the absence of Ca^{2+} was characterized by displacement with a large excess of ATP (Fig. 7*a*). The slow phase of this biphasic reaction had a rate constant of 0.008 s^{-1}, and this accounted for 65% of the observed amplitude. Thus FDP dissociation occurs somewhat faster than the effective turnover rate of FTP by this fraction (measured as 0.0018 s^{-1} for this preparation in an experiment similar to that in Fig. 1*d*), indicating that P_i release (or a conformational change controlling it) is the major rate-limiting stop of the FTPase under relaxing conditions. The fast phase of the displacement reaction (Fig. 7*a*) does not seem to be attributed to the unregulated fraction. Little enhancement in fluorescence is observed for FDP at this controlling it) is the major rate-limiting step of the point), which comprises an exclusively unregulated population, or HMM rendered Ca^{2+}-insensitive by labelling the reactive thiol group (Fig. 10*b* end point). Thus even if FDP binding to the unregulated fraction does occur in the HMM preparation used in Fig. 7, it is likely to be optically silent with respect to formycin fluorescence. The fast phase of FDP displacement (Fig. 7*a*) could arise if there were two classes of binding sites on the regulated fraction. Alternatively the FDP could be distributed between a number of states in slow equilibrium (see the Discussion section).

FDP dissociation in the presence of Ca^{2+} was studied by pre-binding FDP to HMM in the presence of EGTA, then mixing with excess Ca^{2+} (Fig. 7*b*). A decrease in formycin fluorescence occurred with a rate constant of about 5 s^{-1} attributed to FDP release (or a conformational change controlling it) in the presence of Ca^{2+}. Therefore, as with ADP, the rate constant for FDP dissociation from the regulated HMM fraction shows a marked Ca^{2+}-sensitivity, being activated some 600-fold. From comparison with the FTP turnover rate (0.15 s^{-1}), it is apparent that P_i release remains the rate-limiting step after activation by Ca^{2+}.

p[NH]ppF binding and release

The interaction of the non-hydrolysable analogue p[NH]ppF with scallop HMM was studied to explore the mechanism of nucleotide binding further (Fig. 8). p[NH]ppF binding to HMM in the absence of Ca^{2+} gave of the order of a 5-fold enhancement in formycin fluorescence. In the presence of Ca^{2+} a significant enhancement was still observed on p[NH]ppF binding, although this was less at low nucleotide concentrations. Thus, in terms of fluorescence enhancements, p[NH]ppF displayed an intermediate position between FTP and FDP. The kinetics of binding and release of p[NH]ppF were, however, significantly slower than those of FTP and FDP.

The binding of p[NH]ppF was biphasic, the second slow phase being particularly noticeable in the absence of Ca^{2+} and contributing to a greater net enhancement compared with that observed in the presence of Ca^{2+} at low nucleotide concentrations (Figs. 8*a* and 8*b*). On increasing the p[NH]ppF concentration, the rate and the relative amplitude of the first phase increased (Figs. 8*c* and 8*d*). The increase in the overall fluorescence enhancement indicated that the binding constant for p[NH]ppF in the absence of Ca^{2+} was less than 1 μM, whereas in the presence of Ca^{2+} it was about 10 μM. The apparent association rate constant (approx. 2×10^4 $M^{-1} \cdot s^{-1}$) for p[NH]ppF and HMM was two to three orders of magnitude slower than for ATP, reflecting a combined influence of the formycin ring and imidodiphosphate group.

The reverse conformational changes associated with p[NH]ppF dissociation were investigated by displacement with excess ATP and/or Ca^{2+}. In the absence of Ca^{2+} displacement of p[NH]ppF by ATP was biphasic. The first phase, which may be attributed to release from the unregulated fraction, was followed by a very slow process ($t_{\frac{1}{2}} > 1$ h, $k < 10^{-4}$ s^{-1}). The latter was difficult to define accurately because of the aging of the HMM sample at 20 °C and exhaustion of the ATP by the unregulated fraction. In contrast, p[NH]ppF was displaced within minutes when the reaction was performed in the presence of Ca^{2+} (Fig. 9). When p[NH]ppF was pre-bound in EGTA and then displaced by the simultaneous addition of Ca^{2+} and ATP, the fluorescence profile was biphasic (Fig. 9*a*). The phases were studied

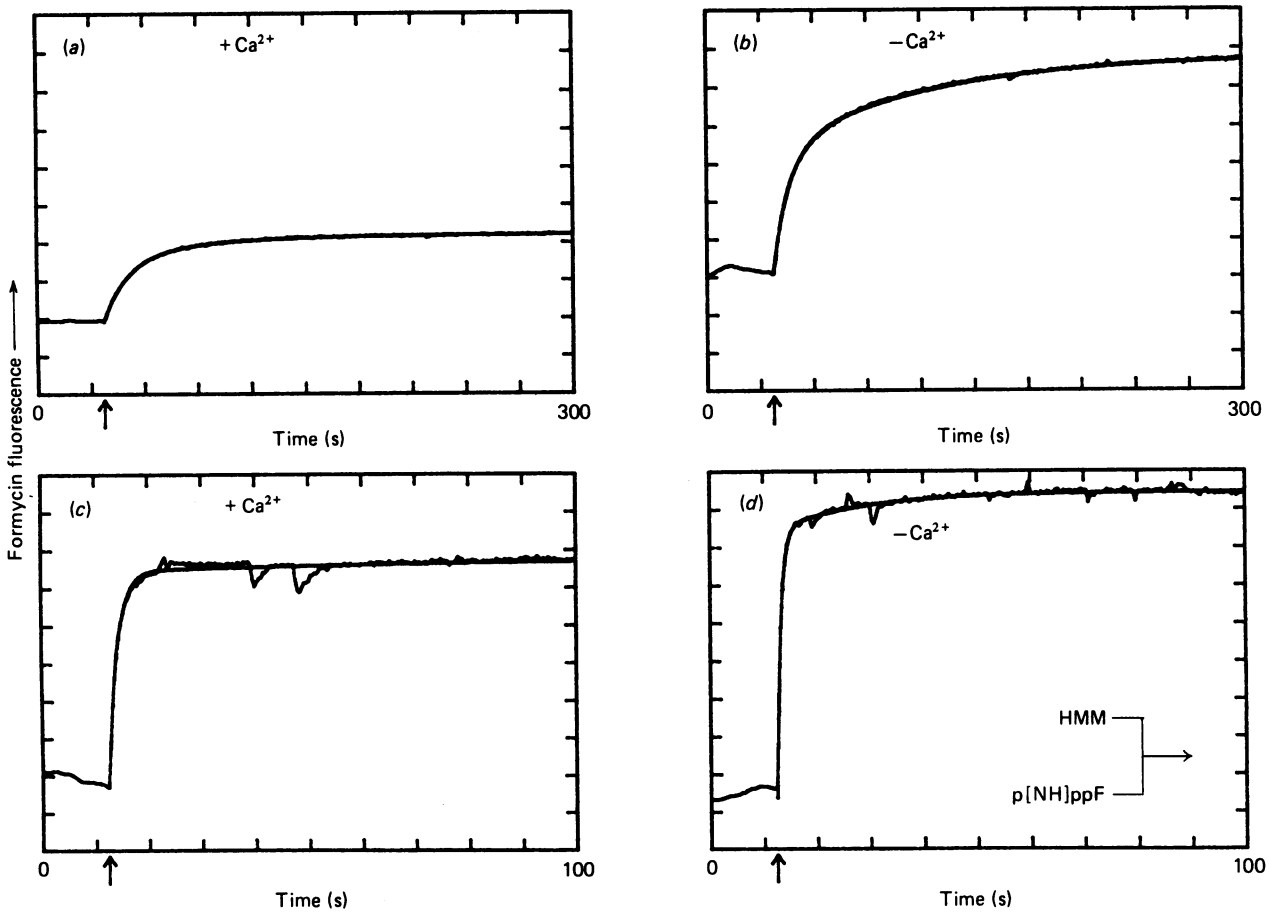

Fig. 8. p[NH]ppF binding to HMM

The stopped-flow records show p[NH]ppF binding to HMM in the absence and in the presence of Ca^{2+}. (*a*) 6 μM-p[NH]ppF was mixed with 4 μM-HMM in the presence of 100 μM free Ca^{2+}. (*b*) 6 μM-p[NH]ppF was mixed with 4 μM-HMM in the presence of 100 μM-EGTA. (*c*) 50 μM-p[NH]ppF was mixed with a 4 μM-HMM in the presence of 100 μM free Ca^{2+}. (*d*) 50 μM-p[NH]ppF was mixed with 4 μM-HMM in the presence of 100 μM-EGTA. Other conditions were as for Fig. 1. Biphasic exponential fits to the traces yielded rate constants and relative amplitudes of (*a*) 0.22 s^{-1} (72%) and 0.053 s^{-1} (28%), (*b*) 0.11 s^{-1} (57%) and 0.012 s^{-1} (43%), (*c*) 0.57 s^{-1} (95%) and 0.015 s^{-1} (5%), and (*d*) 0.41 s^{-1} (88%) and 0.02 s^{-1} (12%). One vertical diversion represents in (*a*) and (*b*) a 10% enhancement and in (*c*) and (*d*) a 2% enhancement relative to the end-point fluorescence.

separately by first mixing with Ca^{2+} alone, which indicated that a conformational transition occurred with a rate constant of 0.12 s^{-1} (Fig. 9*b*). The p[NH]ppF that remained bound to HMM in the presence of Ca^{2+} was then displaced by ATP with a rate constant of 0.05 s^{-1} (Fig. 9*c*).

The detailed analysis of p[NH]ppF binding and release from HMM is complicated by the contribution from the unregulated fraction. Nevertheless the experiments show that Ca^{2+} controls both the formation (Figs. 8*a* and 8*b*) and decay (Fig. 9*b*) of a nucleotide complex that is long-lived under relaxing conditions. In the case of FTP, the effect of Ca^{2+} on the formation of the long-lived complex is not immediately apparent (Fig. 4), although this may be a significant feature of the mechanism (see the Discussion section).

Factors influencing the degree of regulation

The biphasic decay in formycin fluorescence during the turnover of FTP by HMM (Fig.1*d*), in principle, provides a convenient assay to estimate the fraction of regulated and unregulated molecules. Sixteen HMM preparations used for kinetic analysis had an average of 72% (S.D. 7.1%) regulated molecules, as judged by the relative amplitudes of the fast and the slow phases, with the fluorescence level after addition of Ca^{2+} as a baseline (cf. Table 1). The maximum regulated fraction achieved for a bulk preparation was 83%, and the occasional preparations that had less than 60% regulated molecules (presumably owing to over-digestion) were discarded. The FTP turnover assay was used to explore a number of conditions that lead to changes in the degree of regulation.

Treatment of HMM with EDTA, followed by column centrifugation on Bio-Gel P-60, resulted in a significant loss of regulatory light chains (Shpetner, 1986; K. E. Warriner & C. R. Bagshaw, unpublished work). In such preparations the fast phase of FTP turnover predominated. However, it was difficult to effect complete removal of the regulatory light chains and the complete loss of the slow phase by this procedure. In our hands, typically about 20% of the light chains remained. The effect of removal of regulatory light chains was more readily demonstrated with intact myosin (Jackson *et al.*, 1987).

Storage of HMM at 5–10 mg/ml at 4 °C generally was

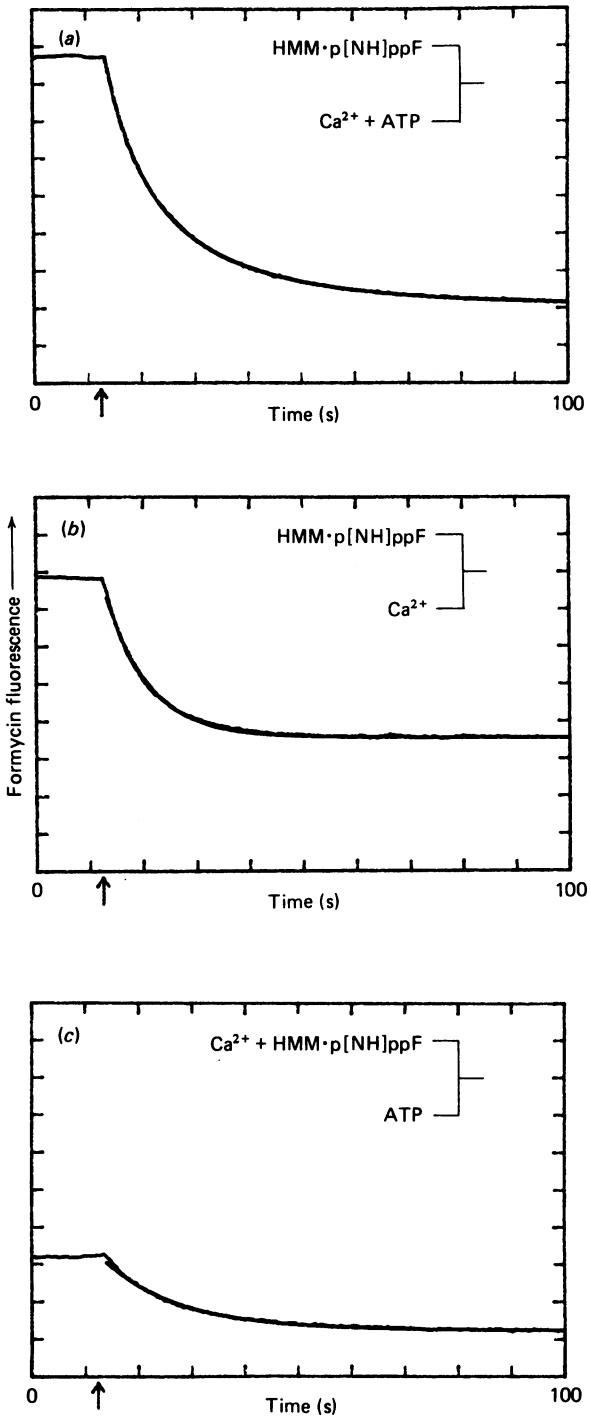

Fig. 9. p[NH]ppF dissociation from HMM in the presence of Ca^{2+}

The stopped-flow records show the dissociation of p[NH]ppF from HMM as monitored by formycin fluorescence. (*a*) One syringe contained 500 μM-ATP and 200 μM-Ca^{2+} and the other 4 μM-HMM, 6 μM-p[NH]ppF and 100 μM-EGTA. (*b*) One syringe contained 200 μM-Ca^{2+} and the other 4 μM-HMM, 6 μM-p[NH]ppF and 100 μM-EGTA. (*c*) One syringe contained 500 μM-ATP and 100 μM-Ca^{2+} and the other 4 μM-HMM, 6 μM-p[NH]ppF and 100 μM-Ca^{2+}. Other conditions were as for Fig. 1. Rate constants of superimposed fits were (*a*) 0.17 s^{-1} and 0.046 s^{-1} (biphasic fit), (*b*) 0.13 s^{-1} and (*c*) 0.07 s^{-1}. One vertical division represents a 6.25% change in fluorescence.

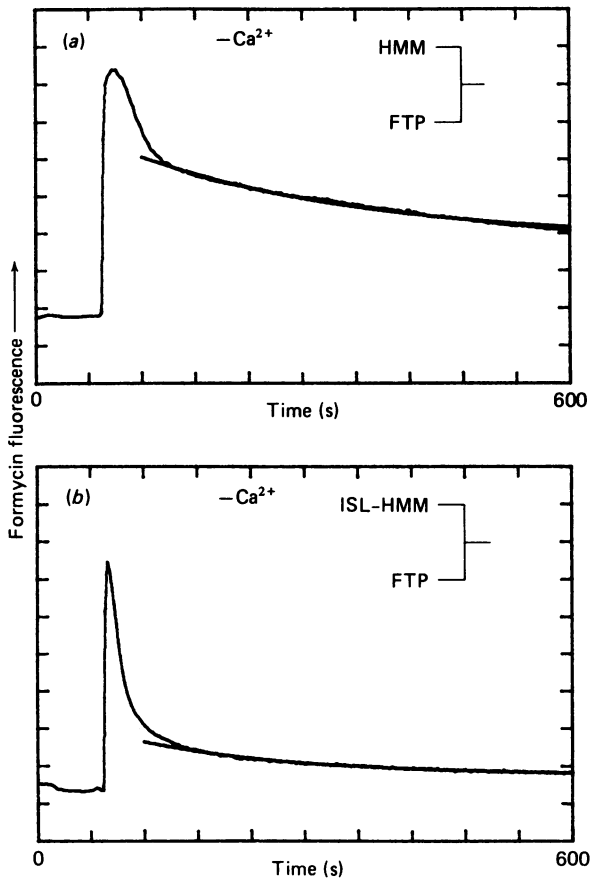

Fig. 10. Effect of labelling HMM with a spin label

The stopped-flow records show FTP turnover by HMM before and after spin-labelling. (*a*) 10 μM-FTP was mixed with 4 μM-HMM. (*b*) 10 μM-FTP was mixed with 4 μM spin-labelled HMM (labelled at 50 μM-HMM with 75 μM-4-(2-iodoacetamido)-2,2,6,6-tetramethylpiperidino-oxyl spin label (ISL) for 100 min. Both reactions were performed in the presence of 100 μM-EGTA. Fits to the slow phase yielded (*a*) 3.8×10^{-3} s^{-1} and (*b*) 5.7×10^{-3} s^{-1}.

accompanied by a slow loss of the regulated fraction. All experiments described above were therefore performed within 2 days of preparation. Rapid freezing in the assay buffer and storage at −20 °C was detrimental to Ca^{2+}-sensitivity of the HMM ATPase. However, storage at −70 °C proved better, one preparation retaining 60% regulated molecules after 10 months.

Previous studies indicated that labelling the heavy-chain reactive thiol group (presumably SH-1) with spectroscopic probes was detrimental to the Ca^{2+}-sensitivity of the actin-activated ATPase (Jackson *et al.*, 1986). Fig. 10 shows that there is a marked loss in amplitude of the slow phase of FTP turnover on reaction with a spin label. Concomitant e.p.r. measurements showed that this change correlated with the rate of incorporation of the spin label. The profile of the FTP turnover indicates that once a thiol group of an HMM head is labelled the ATPase cannot be inhibited by removal of Ca^{2+} (i.e. there is an immediate and more-or-less complete switch to the unregulated state). It is dificult to resolve whether a very limited Ca^{2+}-sensitivity remains (2-fold activation) owing to the ill-conditioned nature of biphasic exponentials (Cornish-Bowden, 1976).

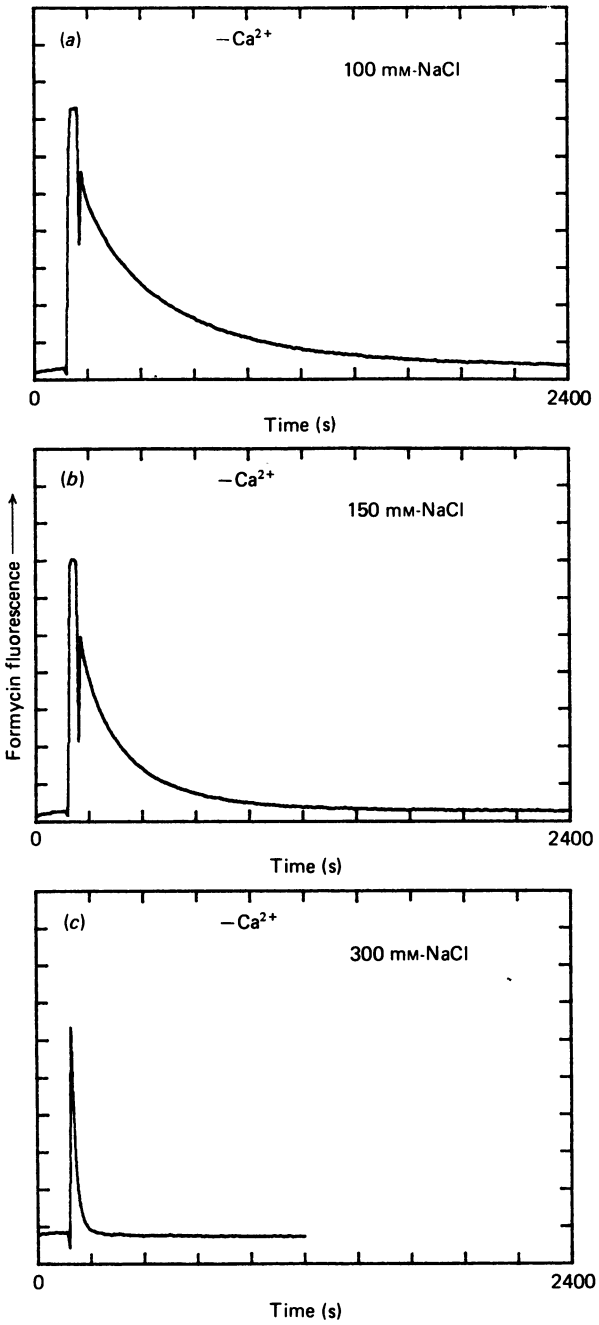

Fig. 11. Effect of [NaCl] on the turnover of FTP by HMM in the absence of Ca^{2+}

Experiments were performed as described for Fig. 3(*b*) with the same HMM preparation. (*a*) 10 μM-FTP was added to 2 μM-HMM in 100 mM-NaCl followed after 60 s by 1 mM-Mg ATP. (*b*) As (*a*), but in 150 mM-NaCl and with MgATP addition after 50 s. (*c*) As (*a*), but in 300 mM-NaCl and with MgATP addition after 20 s. All reactions were performed in the presence of 100 μM-EGTA. The traces were analysed by using a single-exponential or biphasic-exponential fit as summarized in Table 2.

However, it is clear that the spin labels and fluorescent labels investigated so far (Jackson *et al.*, 1986) cannot be used to probe the highly suppressed state, which is of particular interest in the scallop system, when directed to the reactive thiol group (cf. Wells & Bagshaw, 1984*b*).

Raising the ionic strength gave a progressive activation of the rate of FTP turnover by the regulated fraction in the absence of Ca^{2+} (Fig. 11). This was apparent by a gradual increase in the rate of the slow phase. There was also an indication that the amplitude of the slow phase decreased with increasing ionic strength (Table 2), although this could not be determined accurately for higher rates (above 0.01 s^{-1}) owing to the error in defining the start point of the ATP chase by manual mixing methods. In fact, at intermediate [NaCl] the decay profiles showed a small but systematic deviation from a single-exponential fit. When fitted to a biphasic exponential function the relative contribution of the fast phase increased with increasing ionic strength (Table 2). At high ionic strengths (over 500 mM-NaCl) the observed decay profile merged with that attributed to the unregulated fraction and under these conditions no Ca^{2+}-sensitivity was detected (cf. Wells *et al.*, 1985). In the concentration range 0.1–0.4 M sodium acetate was less effective than NaCl in over-riding the trapping of nucleotide during FTP turnover in the absence of Ca^{2+}.

DISCUSSION

FTP has proved to be a useful analogue for the study of the Ca^{2+}-sensitivity of scallop myosin subfragments. Large changes in formycin fluorescence accompany the FTP-binding and product-release steps. This enables the properties of the unregulated and regulated HMM fractions to be resolved during a limited FTP turnover in the absence of Ca^{2+}, in the same way as the turbidity assay was employed to study the actin-activated ATPase (Wells & Bagshaw, 1984*a*). Limited turnovers of FTP are readily performed even in a conventional fluorimeter with manual addition, and allow the fraction of regulated HMM molecules and their relaxed FTPase rate to be determined.

The simplest scheme for the FTPase activity of scallop HMM is given in Scheme 1, to allow comparison with the corresponding pathway proposed for the ATPase mechanism (Jackson & Bagshaw, 1988).

In general, the kinetic constants of the FTPase reaction appear comparable with those of the corresponding ATPase mechanism, apart from an order of magnitude decrease in the association rate constants for nucleotide binding. This characteristic was noted previously for rabbit myosin subfragments (Bagshaw *et al.*, 1972), and might be attributed to the preponderance of the syn conformation of formycin in free solution (Ward & Reich, 1968), whereas the ATPase site is probably complementary to the anti conformation (cf. Shoham & Steitz, 1980).

Apart from the determination of the properties of the FTPase reaction, FTP also proved useful as a displacing agent to characterize some of the elementary steps of the ATPase reaction (Jackson & Bagshaw, 1988). At the concentrations required to achieve efficient competition with bound ATP, a significant change in formycin fluorescence could be detected. This contrasts with our attempts to use chromophoric thionucleotides as displacing agents (cf. Eccleston & Trentham, 1977), where the background absorbance became too high at the nucleotide concentrations required. Unfortunately FTP is not a sufficiently good competitor to chase the $M \cdot ADP \cdot P_i$ species during an ATP turnover. However, the $M \cdot FDP \cdot P_i$ intermediate was readily displaced with an excess of ATP (Fig. 3). These experiments showed

Table 2. Dependence of observed rate constants and amplitudes for FTP turnover by HMM as a function of [NaCl]

Fluorescence profiles of the type shown in Figs. 3(*b*) and 11 were fitted to single-exponential or double-exponential functions. At intermediate [NaCl] concentrations the traces deviated systematically from a single exponential. Fitting to a double-exponential function gave up to a 4-fold decrease in the residual error in these cases. The data could not be analysed accurately at [NaCl] above 300 mM because the first phase became too fast to measure by manual addition and the profile merged with that attributed to the unregulated fraction.

	Single exponential		Double exponential			
[NaCl] (mM)	A (%)*	k (s^{-1})	$A1$ (%)*	$k1$ (s^{-1})	$A2$ (%)*	$k2$ (s^{-1})
20	100	0.0013	–	–	$\geqslant 98$	0.0013
100	82	0.0026	20	0.014	72	0.0023
150	77	0.0046	41	0.011	45	0.0032
200	76	0.0105	74	0.017	20	0.0047
300	53	0.043	$\geqslant 55$	0.054	$\leqslant 3$	0.0045

* Normalized to 100% of amplitude to slow phase observed in 20 mM-NaCl, which itself was 80% of the total amplitude (Fig. 3*b*).

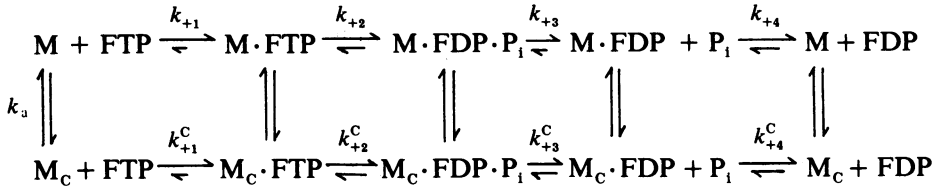

Scheme 1.

M and M_C represent HMM in the absence and in the presence of Ca^{2+} respectively. $k_1 = k_{+1}^C = 2 \times 10^5\ M^{-1} \cdot s^{-1}$, $k_2 \approx k_2^C$ = fast, $k_3 = 0.002\ s^{-1}$, $k_{+3}^C = 0.15\ s^{-1}$, $k_{+4} = 0.008\ s^{-1}$, $k_{+4}^C = 5\ s^{-1}$ and $k_a = 25\ s^{-1}$.

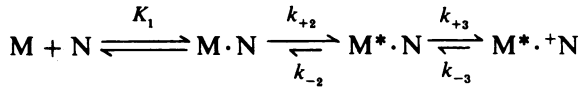

Scheme 2.

that the final turnover of the FTPase by the regulated HMM appears to be no different from that occurring during the steady state and validates the use of single-turnover kinetic analysis.

As with the ATPase mechanism, Scheme 1 is over-simplified in that the nucleotide binding is a multi-step process. Although the reaction profiles of FDP and p[NH]ppF binding (Figs. 5 and 8) appear very different to those of ADP binding (Jackson & Bagshaw, 1988; Fig. 3), this may be due primarily to the initial weaker association step of formycin nucleotides. Consider the three-step mechanism shown in Scheme 2 for nucleotide (N) binding in the absence of Ca^{2+}, in which an asterisk (*) denotes species with enhanced fluorescence. For the case where $k_{+2} + k_{-2} \gg k_{+3} + k_{-3}$ and the first step is a rapid equilibrium, the fluorescence change on binding may appear mono- or bi-phasic, depending on the nucleotide concentration relative to $1/[K_1(1+K_2)]$. The observed rate constants for the two phases are $k_{+2} \cdot K_1 \cdot [N]/(1 + K_1 \cdot [N]) + k_{-2}$ and $k_{+3} \cdot K_1 \cdot [N] \cdot (1 + K_2)/\{1 + K_1 \cdot [N] \cdot (1 + K_2)\} + k_{-3}$. When $[N] \gg 1/[K_1(1+K_2)]$ and $k_{+2} > k_{-2}$, $M^* \cdot N$ will form rapidly and stoichiometrically in a single phase, as described by the first term, and any subsequent transition to $M^* \cdot {}^+N$ will remain optically silent. This would be an appropriate model for the ADP binding for the nucleotide concentration range studied (above 10 μM). In the case of formycin nucleotides, the value of K_1 is lowered by one to two orders of magnitude. As a result, at the intermediate nucleotide concentrations available to investigation (3–75 μM), the formation of $M^* \cdot N$ during the first phase is incomplete and a second phase is observed as the formation of $M^* \cdot {}^+N$ pulls the overall reaction to the right. Increasing [N] results in the increase in the amplitude of the first phase at the expense of the second phase, although the latter will remain to some extent if k_{-2} is comparable with or greater than k_{+2} (step 3 will, of course, only exert an influence if k_{+3} is comparable with or greater than k_{-3}). This mechanism provides a reasonable description of the profiles observed for p[NH]ppF binding, where the second slow phase becomes a minor component when the p[NH]ppF concentration is increased from 3 μM to 25 μM (reaction-chamber concentrations, Fig. 8). Appropriate values for the constants in Scheme 2 are $K_1(1+K_2) = 10^5\ M^{-1}$, $K_1 \cdot k_{+2} = 2 \times 10^4\ M^{-1} \cdot s^{-1}$, $k_{+3} = 0.02\ s^{-1}$ and $k^{-3} = 10^{-4}\ s^{-1}$, giving an overall equilibrium constant of 5×10^{-8} M, in the absence of Ca^{2+}. The complete analysis of p[NH]ppF binding is, however, complicated by the presence of the unregulated fraction of HMM, which is likely to make a larger contribution to the fast phase at higher nucleotide concentrations (assuming that it behaves similarly to the total population in the presence of Ca^{2+}).

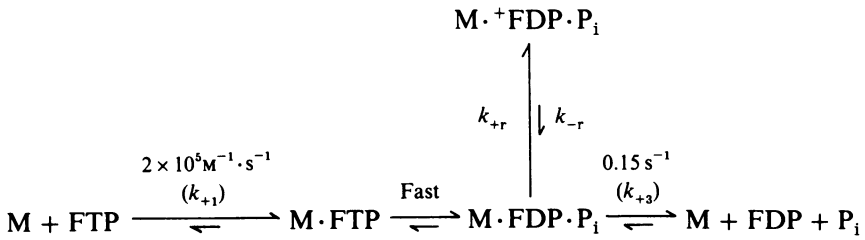

Scheme 3.

The analysis of FDP binding suffers from other difficulties. It is not clear if the slow phase of binding observed at low [FDP] diminishes in amplitude and is replaced by a third faster phase at higher [FDP] or whether the two phases, resolved by the biphasic fit, increase in rate together. Analyses of such profiles are highly susceptible to ill-conditioning (Cornish-Bowden, 1976). It is premature to conclude whether Scheme 2 is a reasonable description of the main features of the FDP-binding reaction. It would account for the biphasic release of bound FDP if k_{+3} and k_{-3} are of comparable magnitude, giving an initial equilibrium mixture of M*·N and M*·$^+$N states. Scheme 2 could generate triphasic profiles on FDP binding if some fluorescence enhancement occurred on formation of the M·N species. On the other hand it is difficult to reconcile the overall apparent binding constant of about 40 μM for FDP (Fig. 6) with the slow dissociation kinetics (Fig. 7*a*), which would lead to lower association rates than are observed ($> 2 \times 10^4$ M$^{-1}\cdot$s^{-1}) at low [FDP]. The possibility of two classes of sites must therefore be considered. Other workers have proposed that HMM from non-myosin-regulated species shows heterogeneity in binding nucleoside diphosphates and imido analogues and have related these observations to asymmetry of the two myosin heads (cf. Schaub & Watterson, 1981). Two classes of site seem necessary to account for the small activation of the overall steady-state rate by FDP, a phenomenon that requires further study by transient-state methods. At this stage in our analysis of the problem it is desirable to stress only those conclusions that are model-independent. That formycin nucleotides become slowly bound to HMM in the absence of Ca^{2+} (at least to a fraction of the sites) is evident from the fluorescence profiles of FDP and p[NH]ppF in Figs. 5 and 8. Addition of Ca^{2+} causes the relatively rapid release from these complexes (Figs. 7 and 9). The enhancement in the rate of the release of nucleotide by Ca^{2+} (two orders of magnitude) may well be greater than the change in the overall equilibrium binding constant, because the relaxed complexes are trapped kinetically rather than thermodynamically.

The slow steps observed with FDP and p[NH]ppF binding raise the question as to whether FTP binding is more complicated than suggested by the fluorescence profiles of Fig. 4. It is possible that there is a moderately slow transition of the products complex, M·FDP·$P_i \rightleftharpoons$ M·$^+$FDP·P_i, in the absence of Ca^{2+} that remains optically silent because the initial reaction steps lead to the full fluorescence enhancement (cf. discussion of Scheme 2 above). Preliminary evidence suggesting that an additional transition exists includes the finding that the residual FTP detected in quench experiments (and assigned to the M·FTP state) decays considerably faster than the turnover rate assigned to the regulated fraction (cf. Bagshaw & Trentham, 1973). Such a transition may occur as an in-line step or as a branch, the latter situation giving rise to a number of interesting properties. It is possible to model the characteristics of FTP turnover in the presence and in the absence of Ca^{2+} by a scheme in which regulation is achieved by trapping the M·$^+$FDP·P_i intermediate on a side branch of the scheme, leaving the rate constants for the in-line steps Ca^{2+}-insensitive (Scheme 3).

Consider the case where $k_{+r} = 50\ k_{-r}$. If $k_{+r} \gg k_{+3}$ then the scheme behaves almost as an in-line mechanism and will not be considered further. If, however, k_{+r} and k_{+3} are of comparable magnitude then, during the first turnover, not all the regulated molecules will trap products in the refractory M·$^+$FDP·P_i state, although they will do so after a few further turnovers (because $k_{+r} \gg k_{-r}$). As a result the amplitude of the phase associated with the regulated fraction will be smaller in a single turnover (i.e. stoichiometrtic [FTP]) compared with a limited turnover (e.g. a 5-fold excess of FTP over total HMM sites as used in our standard assay). We have observed this phenomenon in a number of experiments. With respect to the results described in the current work, Scheme 3 can account for the partial loss of amplitude as well as the increase in the rate of the slow phase with increasing ionic strength (cf. Table 2). If high [NaCl] decreases k_{+r} and increases k_{-r}, then only a fraction $[k_{+r}/(k_{+r}+k_{-r})]$ of the regulated population will appear to trap products in the M·$^+$FDP·P_i state. The branched scheme of Scheme 3 cannot alone account for the phases that we have attributed to the regulated and unregulated fractions at low ionic strength, where it is still necessary to include 25% Ca^{2+}-insensitive molecules. It does, however, emphasize the caution required in using the relative amplitudes of the fast and the slow phases as a measure of the regulated fraction at increased ionic strengths. According to Scheme 3, activation of the FTPase by Ca^{2+}, removal of regulatory light chains, high ionic strength or labelling the reactive thiol group would be accounted for by a reduction in the equilibrium constant, K_r, so that little or no product trapping occurs. The production of the trapped complex at only a moderate rate constant ($k_{+r} = 0.15$ s^{-1}) might account for the delay in relaxation of rigour tension when caged ATP was photolysed in scallop muscle fibres in the absence of Ca^{2+} (Hibberd *et al.*, 1983).

The multi-step nature of nucleotide binding also raises the question as to whether the complex M*·$^+$N, which exhibits a slow release of FDP, is on the kinetic pathway of FTP turnover or is a branch complex. The rate constant for this process (0.008 s^{-1}) is sufficiently fast for it to be an in-line intermediate, but the two models are not readily distinguished (cf. rabbit myosin ATPase, where a kinetic test was devised; Bagshaw & Trentham,

1974). In other cases certain myosin–nucleoside diphosphate complexes have been characterized that are kinetically incompetent to be in-line intermediates (Goody & Hofmann, 1980).

The kinetic findings above, in conjunction with structural studies (Vibert *et al.*, 1986; Rüegg, 1986), are beginning to expose the underlying mechanism of myosin-linked regulation. The sequence of events is better considered in terms of relaxation rather than activation, since the latter is effectively de-inhibition of the regulatory system. Ca^{2+} removal from a site (possibly the essential light chain; Collins *et al.*, 1986) on the regulatory domain is rapid (Jackson & Bagshaw, 1988) and leads to the relative movement of the regulatory and essential light chains (Hardwicke *et al.*, 1983). This conformational change is transmitted to the ATPase site located towards the middle of the head (Munson *et al.*, 1986). The finding that the essential light chain of vertebrate smooth-muscle myosin extends to the active site is obviously pertinent to this mechanism (Okamoto *et al.*, 1986). However, the regulatory light chains are vital to this communication, since their removal results in permanent activation of both the actin-activated (Kendrick-Jones *et al.*, 1976) and the intrinsic myosin ATPase (Ashiba *et al.*, 1980; Wells *et al.*, 1985; Jackson *et al.*, 1987). The heavy chain itself is also important, since cleavage at the neck region to yield S1 or labelling of the reactive thiol group prevents communication (Fig. 10; Jackson *et al.*, 1986; Titus & Szent-Györgyi, 1986). The ultimate effect of this message on the active site is to trap the myosin-products complex $M \cdot ADP \cdot P_i$ (or $M \cdot FDP \cdot P_i$) in a state that interacts weakly with actin (Wells & Bagshaw, 1984*a*, 1985). Since Ca^{2+} appears to have little effect on the binding of actin as such (Chalovich *et al.*, 1984; Stanners & Bagshaw, 1987), it follows that product release from the actin $\cdot M \cdot ADP \cdot P_i$ complex must also be markedly suppressed in the relaxed state.

The trapping of products by myosin is primarily a kinetic rather than a thermodynamic phenomenon. It is unlikely that the observed rate constant of P_i release of $0.002\ s^{-1}$ reflects a single event as modelled by step 3 in Scheme 1 or step r in Scheme 3. Rather, it might be envisaged that the myosin active site undergoes a number of rapid breathing motions (Prince *et al.*, 1981) and P_i is released when all the motions, by chance, give rise to an open conformation (e.g. ten independent motions, each existing in an open conformation for one-tenth of the time, could combine to yield a net fractional time of opening of 10^{-10}). In this way, the microsecond time scale of domain motions could give rise to product release over a period of minutes. A consequence of this mechanism is that only a small change in the frequency of the fundamental motions is required to yield a large amplification in the overall rate of product release (e.g. increasing the individual fractional opening times by 2-fold gives a 10^3-fold increase in the net opening time for the example above). Regulation via internal head motions has also been considered by Vibert *et al.* (1986) on the basis of the multidomain nature of the myosin head, which is gradually becoming apparent from limited proteolysis and electron microscopy.

Electron microscopy has revealed that, under relaxing conditions ($-Ca^{2+}$, $+ATP$), the cross-bridges of native scallop myosin filaments take on a highly ordered appearance (Vibert & Craig, 1985). Addition of Ca^{2+} or removal of ATP leads to a disordered structure. Of particular interest is the finding that Ca^{2+} induces a rapid change in structure, whereas ATP removal requires some 30 min to have an effect. These observations fit in well with our studies of the corresponding reactions with HMM in solution. In combining structural and kinetic data, it would be desirable to explore the regulation of ATPase activity of intact myosin in the filamentous state. Recently we have succeeded in recording the formycin fluorescence profile during the turnover of FTP by myosin filaments in suspension (Jackson *et al.*, 1987). These studies confirm that the ATPase mechanism deduced from HMM is applicable to intact myosin and open up a wide range of experiments to further the understanding of myosin-linked regulation in molluscan systems. In addition, FTP has proved useful for investigating trapped species in other types of myosin. Cross *et al.* (1986) reported that the products of ATP hydrolysis become trapped during the 6 S to 10 S transition of vertebrate smooth muscle. Formycin fluorescence provides a convenient assay for this system (R. A. Cross, A. P. Jackson & C. R. Bagshaw, unpublished work), where the half-life of the nucleotide complex is of the order of 70 min.

We are grateful to Dr. J. F. Eccleston for advice on nucleotide probes and Professor M. C. R. Symons for use of the e.p.r. spectrometer. We thank Professor A. G. Szent-Györgyi, Dr. A. R. Walmsley and Karen Warriner for discussions and the Science and Engineering Research Council for financial support.

REFERENCES

Ashiba, G., Asada, T. & Watanabe, S. (1980) J. Biochem. (Tokyo) **88**, 837–846

Bagshaw, C. R. (1974) Ph.D. Thesis, University of Bristol

Bagshaw, C. R. & Trentham, D. R. (1973) Biochem. J. **133**, 323–328

Bagshaw, C. R. & Trentham, D. R. (1974) Biochem. J. **141**, 331–349

Bagshaw, C. R., Eccleston, J. F., Trentham, D. R., Yates, D. W. & Goody, R. S. (1972) Cold Spring Harbor Symp. Quant. Biol. **37**, 127–135

Bagshaw, C. R., Eccleston, J. F., Eckstein, F., Goody, R. S., Gutfreund, H. & Trentham, D. R. (1974) Biochem. J. **141**, 351–364

Chalovich, J. M., Chantler, P. D., Szent-Györgyi, A. G. & Eisenberg, E. (1984) J. Biol. Chem. **259**, 2617–2621

Collins, J. H., Jakes, R., Kendrick-Jones, J., Leszyk, J., Barouch, W., Theibert, J. L., Spiegel, J. & Szent-Györgyi, A. G. (1986) Biochemistry **25**, 7651–7656

Cornish-Bowden, A. (1976) Principles of Enzyme Kinetics, pp. 154–155, Butterworths, London and Boston

Cross, R. A., Cross, K. E. & Sobieszek, A. (1986) EMBO J. **5**, 2637–2641

Eccleston, J. F. & Trentham, D. R. (1977) Biochem. J. **163**, 15–19

Ferenczi, M. A. (1978) Ph.D. Thesis, University of London

Goody, R. S. & Hofmann, W. (1980) J. Muscle Res. Cell Motil. **1**, 101–115

Hardwicke, P. D. M., Wallimann, T. & Szent-Györgyi, A. G. (1983) Nature (London) **301**, 478–482

Hibbard, M. G, Goldman, Y. E. & Trentham, D. R. (1983) in Biological Structures and Coupled Flows (Oplatka, A. & Balaban, M., eds.), pp. 223–238, Academic Press, New York and Philadelphia

Itaya, K. & Ui, M. (1966) Clin. Chim. Acta **14**, 361–366

Jackson, A. P. & Bagshaw, C. R. (1988) Biochem. J. **251**, 515–526
Jackson, A. P., Warriner, K. E., Wells, C. & Bagshaw, C. R. (1986) FEBS Lett. **197**, 154–158
Jackson, A. P., Warriner, K. E. & Bagshaw, C. R. (1987) Biochem. Soc. Trans. **15**, 900–901
Kendrick-Jones, J., Szentkiralyi, E. M. & Szent-Györgyi, A. G. (1976) J. Mol. Biol. **104**, 747–775
Munson, K. B., Smerdon, M. J. & Yount, R. D. (1986) Biochemistry **25**, 7640–7650
Okamoto, Y., Sekine, T., Grammer, J. & Yount, R. G. (1986) Nature (London) **324**, 78–80
Prince, H. P., Trayer, H. R., Henry, G. D., Trayer, I. P., Dalgarno, D. C., Levine, B. A., Cary, P. D. & Turner, C. (1981) Eur. J Biochem. **121**, 213–219
Rodbell, M., Birnbaumer, L., Poh, S. L. & Krans, H. M. J. (1971) J. Biol. Chem. **246**, 1877–1882
Rossomando, E. G., Jahngen, J. H. & Eccleston, J. F. (1981) Anal. Biochem. **116**, 80–88
Rüegg, J. C. (1986) Zoophysiology, vol. 19: Calcium in Muscle Activation: A Comparative Approach, Springer-Verlag, Berlin, Heidelberg, New York, London, Paris and Tokyo
Schaub, M. C. & Watterson, J. G. (1981) Biochimie, **63**, 291–299
Shoham, M. & Steitz, T. A. (1980) J. Mol. Biol. **140**, 1–14
Shpetner, H. (1986) Ph.D. Thesis, Brandeis University
Stanners, P. J. & Bagshaw, C. R. (1987) Biochem. Soc. Trans. **15**, 901–903
Titus, M. A. & Szent-Györgyi, A. G. (1986) Biophys. J. **49**, 187a
Trentham, D. R., Eccleston, J. F. & Bagshaw, C. R. (1976) Q. Rev. Biophys. **9**, 217–281
Trybus, K. M. & Taylor, E. W. (1982) Biochemistry **21**, 1284–1294
Vibert, P. & Craig, R. (1985) J. Cell Biol. **101**, 830–837
Vibert, P., Szentkiralyi, E. Hardwicke, P., Szent-Györgyi, A. G. & Cohen, C. (1986) Biophys. J. **49**, 131–133
Ward, D. C. & Reich, E. (1968) Proc. Natl. Acad. Sci. U.S.A. **61**, 1494–1501
Ward, D. C., Reich, E. & Stryer, L. (1969*a*) J. Biol. Chem. **244**, 1228–1237
Ward, D. C., Cerami, A., Reich, E. Acs, G. & Altwerger, L. (1969*b*) J. Biol. Chem. **244**, 3243–3250
Wells, C. & Bagshaw, C. R. (1983) J. Mol. Biol. **164**, 137–157
Wells, C. & Bagshaw, C. R. (1984*a*) FEBS Lett. **168**, 260–264
Wells, C. & Bagshaw, C. R. (1984*b*) J. Muscle Res. Cell Motil. **5**, 97–112
Wells, C. & Bagshaw, C. R. (1985) Nature (London) **313**, 696–697
Wells, C., Warriner, K. E. & Bagshaw, C. R. (1985) Biochem. J. **231**, 31–38
White, D. C. S., Zimmerman, R. W. & Trentham, D. R. (1986) J. Muscle Res. Cell Motil. **7**, 179–192
Yount, R. G., Ojala, D. & Babcock, D. (1971) Biochemistry **10**, 2490–2496

Received 24 April 1987/14 October 1987; accepted 14 December 1987